Journal of Geophysical Research
October 2007; VOLUME 112 (C10002) : 12 Pages
http://dx.doi.org/10.1029/2006JC004010

Importance of the sea surface curvature to interpret the normalized radar cross section

A. A. Mouche[1, 3], B. Chapron[1], N. Reul[1, *], D. Hauser[2], Y. Quilfen[1]

[1]Laboratoire d'Océanographie Spatiale, Ifremer, Plouzané, France
[2]Centre d'Etude des Environnements Terrestre et Planétaires, IPSL, CNRS/UVSQ, Vélizy, France
[3]Also at Centre National d'Etudes Spatiales, Paris, France.

*: Corresponding author : N. Reul, email address : nreul@ifremer.fr

Abstract:

Asymptotic models (small perturbation and small slope approximation at first-order, Kirchhoff approximation or two-scale model) used to predict the normalized radar cross section of the sea surface generally fail to reproduce in detail backscatter radar measurements. In particular, the predicted polarization ratio versus incidence and azimuth angles is not in agreement with experimental data. This denotes the inability of these standard models to fully take into account the roughness properties with respect to the sensor's configuration of measurement (frequency, incidence, and polarization). On the basis of particular assumptions, to decompose the scattered electromagnetic field between zones covered with freely propagating waves and others where roughness and slopes are enhanced, recent works were able to match observations. In this paper, we do not assume such a decomposition but study the latest improvements obtained in the field of approximate scattering theories of random rough surfaces using the local and resonant curvature approximations. These models are based on an extension of the Kirchhoff Approximation up to first order to relate explicitly the curvature properties of the sea surface to the polarization strength of the scattered electromagnetic field. Consistency with previous approaches is discussed. As shown, dynamically taking into account the sea surface curvature properties of the surface is crucial to better interpret normalized radar cross-section and polarization ratio sensitivities to both sensor characteristics and geophysical environment conditions. The proposed developments, termed the Resonant Curvature Approximation (RCA), are found to reproduce experimental data versus incidence angle and azimuth direction. The polarization sensitivity to the wind direction and incidence angle is largely improved. Finally, Gaussian statistical assumption adopted to derive the analytical expression of the normalized radar cross section is also discussed. In particular, the third-order cumulant function is shown to better reproduce the second-order up-/down-wind azimuth modulation. The proposed developments appear very promising for improvement of our understanding and analysis of both sea surface radar backscatter and Doppler signals.

Keywords: Resonant Curvature Approximation; sea surface radar; backscatter.

1. Introduction

As the capabilities of remote sensing instruments ever-increase, new opportunities to develop consistent inversion schemes of the sea surface geometry and kinematic appear. For instance, the high resolution SAR images are now commonly used to retrieve wind fields thanks to the backscattered intensity power [*Monaldo and Kerbaol*, 2003] or the sea surface velocity using the Doppler anomaly analysis [*Chapron et al.*, 2003, 2005]. Consequently, one could think about consistent inversion merging these two sources of information. To resolve the remaining ambiguities in the normalized radar cross-section (NRCS) interpretation. In particular, it will help to better decipher between wind effects and current impacts on the apparent surface roughness.

However, to date, large discrepancies between observations and model predictions still remain. Asymptotic theories as the Small Slope Approximation (SSA) [*Voronovich*, 1994; *Plant*, 2002], Kirchhoff Approximation (KA), or more standard approaches as the Two-Scale Model (TSM) [*Plant*, 1986; *Thompson*, 1988; *Romeiser et al.*, 1997] and the Small Perturbation Method at first order (SPM-1) [*Valenzuela*, 1978] fail to correctly predict the NRCS in both HH and VV co-polarizations under all environmental conditions and sensor configurations and characteristics. Data comparisons by several authors systematically recall these weaknesses. The above cited models cannot reproduce the NRCS in both VV and HH polarizations with respect of incidence angle (see e.g. [*Voronovich and Zavarotny*, 2001; *Kudryavtsev et al.*, 2003; *Plant*, 2003; *Mouche et al.*, 2006b]). Data acquired simultaneously for both co-polarizations help to study more precisely the polarization ratio (PR) defined as the ratio of the NRCS in VV over the NRCS in HH. *Mouche* *et al.* [2005] show that in C-band the PR is azimuth dependent with respect to the wind direction. In C-band, this dependency was clearly evidenced for incidence larger than 30°. *Mouche et al.* [2006b] show that the first order expansion of the Small Slope Approximation (SSA-1) or TSM fail to reproduce this azimuth dependency. By construction SSA-1, SPM-1 and KA cannot reproduce any azimuthal variation for the PR. This is a strong limitation of such models. In opposite, TSM can lead to an azimuth dependency, but generally not in agreement with the data. This difference between TSM and other cited models clearly results from the efforts made in the TSM formalism to take into account the depolarization effects of the largest waves on the Bragg resonant waves (e.g. [*Plant*, 1986; *Thompson*, 1988; *Romeiser et al.*, 1997; *Valenzuela*, 1978]). However, as often discussed, TSM's formalism is somehow arbitrary to the choice of the parameter separating large modulating and small modulated waves. To overcome these issues and to propose consistent inversion schemes, one certainly need to advance in the field of approximate theories of scattering from random rough surface [*Elfouhaily and Guérin*, 2004].

In particular, *Elfouhaily et al.* [2003a] proposed a new asymptotic theory for wave scattering from rough surface taking into account the curvature effect of the surface on the scattered field. This curvature effect is a first order correction term of the zeroth order expression of the scattered field given by the Kirchhoff Approximation (KA). The Local Curvature Approximation (LCA-1) formalism has the advantage to dynamically reach both KA and the Small Perturbation Method at first order (SPM-1) depending upon the surface properties. *Mouche et al.* [2006a] applied LCA-1 to the problem of microwave scattering from ocean surface. Based on analytical comparisons with the Two-Scale Model but also data comparisons, it was shown that LCA-1 polarization sensitivity was very close to TSM and thus somehow inadequate to reproduce the NRCS of the ocean surface. But, in comparison with the TSM, LCA-1 solution is more general as it unifies dynamically SPM and KA asymptotic solutions and removes the issue concerning the dividing scale of the surface. Based on this analysis, a new asymptotic solution which provides a more realistic polarization sensitivity than LCA-1 has been proposed to restrict the curvature correction to the so-called resonant Bragg waves. This model, namely the Resonant Curvature Approximation (RCA), conserves the dynamical properties of LCA-1 to reach KA and SPM-1 asymptotic solution. Accordingly, the polarization ratio at a given incidence angle will be sea surface roughness dependant.

In this paper, we first expose the remaining issues in the field of the sea surface NRCS prediction. Data and model comparisons are presented to illustrate our comments. Then, we briefly present the asymptotic solutions based on the extension of the KA to take into account the surface curvature effect of depolarization for the incident electromagnetic waves. Comparisons between the model and radar data help to discuss the importance of the sea curvature for backscattered signal interpretation. The issue about the statistical representation of the sea surface is also commented to resolve the up/down-wind asymmetry of the observed NRCS. Our conclusions and perspectives for the use of these models in the field of ocean remote sensing ends this work.

2. Position of the problem

To date, there is no electromagnetic model able to reproduce the NRCS in both VV and HH polarizations for all incidence angles, radar wavelength and wind conditions (speed, direction). In particular, the polarization sensitivity is not correctly reproduced. Figure 1 illustrates this point with two examples of PR in Ku and C band. The PR is defined as the ratio of the NRCS in VV over the NRCS in HH polarization. On figure 1 (a), we present the PR versus incidence angle calculated from Ku-band NRCS in both VV and HH polarizations measured by NSCAT. The data acquired in Ku-band were already presented by *Quilfen et al.* [1999]. We consider incidence angles from 20° to 50°. a_0^{pp} stands for the coefficient of the standard three-term Fourier model used for empirical formulations of the NRCS versus viewing angle with respect to wind direction:

$$\sigma_0^{pp}(U,\theta,\Phi) = a_0^{pp}(U,\theta) + a_1^{pp}(U,\theta)\cos(\Phi) + a_2^{pp}(U,\theta)\cos(2\Phi), \tag{1}$$

where U is the near-surface wind speed, θ the radar's incidence angle and Φ the wind direction relative to the radar's azimuth look direction. pp denotes the co-polarization considered. With radar data, model predictions given by SPM-1, TSM, KA and SSA-1 are presented. The sea surface description is given by the unified spectrum for short and long wind driven waves proposed by *Elfouhaily et al.* [1997]. To be consistent with these observations, we consider only the isotropic part of the spectrum. Analytical NRCS expressions of this models are recalled in the appendix. SPM-1 and TSM predictions are only presented for incidence angles greater than 20° as they are not valid for lower incidences. As already reported (see e.g., review by *Valenzuela* [1978]; *Kudryavtsev et al.* [2003]), SPM-1 underestimates the NRCS in HH polarization whereas it is rather good for the VV polarization. The direct consequence is an overestimation of the PR. Adding a modulation from the longer waves to the resonant Bragg waves (which provide SPM-1 backscattering) through a TSM enables to better reproduce the depolarization effect on the predicted NRCS. Yet, NRCS in HH polarization is found lower than the measurements and TSM's PR is not in agreement with the data. As KA does not provide any polarization sensitivity, it is clear that it cannot match the data in VV or HH polarizations for the largest incidence angles where there is a significant polarization difference between the backscattered signal in co-polarizations. SSA-1, by construction, imposes a polarization sensitivity too strong. This comes from the fact that as the incidence angle increases, SSA-1 tends very quickly to the SPM-1 asymptotic solution. To lower this effect, higher orders of SSA must be considered. However, *Voronovich and Zavarotny* [2001] showed that the addition of the second order is not sufficient to reproduce data. The conclusion of these comparisons is that none of the model presented above is able to predict the correct polarization sensitivity versus incidence angle in term of mean level.

On figure 1 (b), we present the PR versus azimuth angle obtained from the NRCS in both VV and HH polarizations measured by the STORM radar. This data acquired in C-band were already presented by *Mouche et al.* [2006b]. A complete presentation of the radar could be found in [*Hauser et al.*, 2003]. We consider a 40° incidence angle and a 11m/s wind speed. Obviously, none of the model is able to reproduce the observed azimuthal PR modulation. As observed, the PR is dependent on geophysical parameters such as the wind direction. Necessarily, the PR expression given by an asymptotic model must be thus sensitive to the sea surface roughness description. This points out the limitations of the above cited models for the understanding of the scattering processes at the sea surface and the development of consistent inversion scheme to retrieve geophysical parameters.

Taking into account these limitations in existing models, we propose to apply two extended versions of the Kirchhoff Approximation model based on a first order correction attributed to the surface curvature.

3. Extended Kirchhoff model for the Normalized Radar Cross Section

3.1. Coordinates system and definitions

To expose the general scattering problem, we adopt the same vectorial conventions than used by *Elfouhaily and Guérin* [2004] in their review on electromagnetic scattering theories. The right cartesian coordinate system is defined by the triplet of normalized vectors $(\hat{x}, \hat{y}, \hat{z})$, where the z-axis is directed upward. Σ is the rough surface which separates the upper medium and the lower medium (respectively air and water in our specific case). The (sea) surface elevation is represented by $z = \eta(x, y) = \eta(\boldsymbol{r})$, where $\boldsymbol{r}$ is the horizontal component of the three-dimensional position wave vector $\boldsymbol{R} = (\boldsymbol{r}, z)$. According to these conventions, we consider a incident downward propagating electromagnetic plane wave with a wave-vector $\boldsymbol{K}_0 = (\boldsymbol{k}_0, -q_0)$. The up-going scattered waves is characterized by the wave-vector $\boldsymbol{K} = (\boldsymbol{k}, q_k)$. $\boldsymbol{k}_0$ and $\boldsymbol{k}$ are the horizontal components of the incident and scattered waves whereas q_0 and q_k are the vertical ones. We define also $\boldsymbol{Q}_h$ and Q_z related to the coordinates of the wave numbers $\boldsymbol{K}$ and $\boldsymbol{K}_0$: $\boldsymbol{Q}_h = \boldsymbol{k} - \boldsymbol{k}_0$ and $Q_z = q_0 + q_k$.

The scattered field above and far away $(R \to \infty)$ from the sea surface is assumed to be related to the incident wave through the relation:

$$\boldsymbol{E}_s(\vec{R}) = -2i\pi \frac{e^{iKR}}{R} \mathbb{S}(\boldsymbol{k}, \boldsymbol{k}_0) \cdot \hat{E}_0. \tag{2}$$

$\mathbb{S}(\boldsymbol{k}, \boldsymbol{k}_0)$ is the so-called scattering operator. $\boldsymbol{E}_s(\boldsymbol{R})$ and $\mathbb{S}(\boldsymbol{k}, \boldsymbol{k}_0)$ can be decomposed on the fundamental polarization basis:

$$\boldsymbol{p}_v^{\pm}(\pm k) = \frac{k\hat{z} \mp q_k \hat{k}}{K} \qquad \boldsymbol{p}_h^{\pm}(\pm k) = \hat{z} \times \hat{k}, \tag{3}$$

where the subscripts v and h indicate the vertical and horizontal polarizations, respectively. The minus superscript corresponds to the down-going plane waves while the plus superscript to the up-going waves. In this vectors basis, the scattering operator is related to the scattering amplitude 2×2 matrix through:

$$\mathbb{S}(\boldsymbol{k}, \boldsymbol{k}_0) = \begin{bmatrix} \boldsymbol{p}_v^-(\boldsymbol{k}_0) \\ \boldsymbol{p}_h^-(\boldsymbol{k}_0) \end{bmatrix}^T \cdot \begin{bmatrix} S_{vv}(\boldsymbol{k}, \boldsymbol{k}_0) & S_{vh}(\boldsymbol{k}, \boldsymbol{k}_0) \\ S_{hv}(\boldsymbol{k}, \boldsymbol{k}_0) & S_{hh}(\boldsymbol{k}, \boldsymbol{k}_0) \end{bmatrix} \cdot \begin{bmatrix} \boldsymbol{p}_v^+(\boldsymbol{k}) \\ \boldsymbol{p}_h^+(\boldsymbol{k}) \end{bmatrix}, \tag{4}$$

where the superscript T stands for the transpose operator. In the 2×2 matrix, the first subscript indicates the incident polarization whereas the second one indicates the scattered polarization configuration considered.

For a given polarization configuration pq, $\mathbb{S}^{pq}(\boldsymbol{k}, \boldsymbol{k}_0)$ is further written as:

$$\mathbb{S}^{pq}(\boldsymbol{k}, \boldsymbol{k}_0) = \frac{1}{Q_z} \int_{\boldsymbol{r}} \mathbb{N}^{pq}(\boldsymbol{k}, \boldsymbol{k}_0; \eta(\boldsymbol{r})) e^{-iQ_z \eta(\boldsymbol{r})} e^{-i\boldsymbol{Q}_H \cdot \boldsymbol{r}} d\boldsymbol{r}, \tag{5}$$

where $\mathbb{N}^{pq}(\boldsymbol{k}, \boldsymbol{k}_0; \eta(\boldsymbol{r}))$ is a Kernel depending on the approach considered to establish the solution.

The scattering cross-section is given by the incoherent second order statistical expression:

$$\sigma^{pq} =< |\mathbb{S}^{pq}(\boldsymbol{k}, \boldsymbol{k}_0)|^2 > -| < \mathbb{S}^{pq}(\boldsymbol{k}, \boldsymbol{k}_0) > |^2 \tag{6}$$

3.2. Local and Resonant Curvature Approximations

Based on the work performed by *Elfouhaily et al.* [2003b], *Elfouhaily et al.* [2003a] expanded the scattering matrix up to the first order such as:

$$\begin{aligned} \mathbb{S}^{pq}(\boldsymbol{k}, \boldsymbol{k}_0) \;&=\; \frac{\mathbb{K}(\boldsymbol{k}, \boldsymbol{k}_0)}{Q_z} \int_{\boldsymbol{r}} e^{-iQ_z \eta(\boldsymbol{r})} e^{-i\boldsymbol{Q}_H \cdot \boldsymbol{r}} d\boldsymbol{r} \\ &- \mathrm{i} \int_{\boldsymbol{r}} \int_{\boldsymbol{\xi}} T(\boldsymbol{k}, \boldsymbol{k}_0; \boldsymbol{\xi}) \hat{\eta}(\boldsymbol{\xi}) e^{-iQ_z \eta(\boldsymbol{r})} e^{-i(\boldsymbol{Q}_H - \boldsymbol{\xi}) \cdot \boldsymbol{r}} d\boldsymbol{\xi} d\boldsymbol{r}, \end{aligned} \tag{7}$$

where

$$T_{\mathrm{lca}}(\boldsymbol{k}, \boldsymbol{k}_0; \boldsymbol{\xi}) = [\mathbb{B}(\boldsymbol{k}, \boldsymbol{k}_0; \boldsymbol{\xi}) - \mathbb{K}(\boldsymbol{k}, \boldsymbol{k}_0)], \tag{8}$$

is a kernel defined to take into account the surface curvature effects on the scattered field. $\mathbb{B}$ is the Bragg Kernel and $\mathbb{K}$ is the Kirchhoff Kernel (see e.g. *Elfouhaily et al.* [2003a] for their analytical expression). In Eq.(), the second term represents a first order correction to KA given by the first term. This first order curvature term has the property to reach dynamically both KA and SPM-1 limits with respect to the frequency and the properties of the surface considered. $\hat{\eta}(\boldsymbol{\xi})$ is the Fourier transform of the surface height function $\eta(\boldsymbol{r})$, $\boldsymbol{\xi}$ the wave-number of the surface in the spectral domain.

In [*Mouche et al.*, 2006a], we showed that we could choose a formulation for this Kernel which conserves all the dynamic properties of this proposed solution but with a weaker polarization sensitivity, considering only the curvature effect of the resonant Bragg waves. In this case, the Kernel expression is:

$$T_{\mathrm{rca}}(\boldsymbol{k},\boldsymbol{k}_0;\boldsymbol{\xi}) = [\mathbb{B}(\boldsymbol{k},\boldsymbol{k}_0;\boldsymbol{\xi}) - \mathbb{K}(\boldsymbol{k},\boldsymbol{k}_0)]\delta(\boldsymbol{\xi} - \boldsymbol{Q}_H). \tag{9}$$

As already discussed by *Mouche et al.* [2006a], this solution can be compared with the improved Green's function method proposed by *Shaw and Dougan* [1998] excepted that the formulation helps to preserve the required shift and tilt invariance properties due to the LCA-1-like formalism of the RCA solution.

Assuming Gaussian statistics for the sea surface description, the derivation of the NRCS using the scattering matrix expansion up to the first order for any expansion such as $\mathbb{N}^{pq}(\boldsymbol{k}_0,\boldsymbol{k}) = \mathbb{N}_0^{pq}(\boldsymbol{k}_0,\boldsymbol{k}) + \int_{\boldsymbol{\xi}} N_1^{pq}(\boldsymbol{k}_0,\boldsymbol{k};\boldsymbol{\xi})\hat{\eta}(\boldsymbol{\xi})e^{i\boldsymbol{\xi}\cdot\boldsymbol{r}}d\boldsymbol{\xi}$ was already done and discussed in the context of LCA/RCA models by *Mouche et al.* [2006a]. In the case of microwave scattering from the sea surface sea surface, it was concluded that the predicted NRCS is very similar than the one using the phase perturbation method firstly proposed by *Berman and Dacol* [1990] and then applied by *Voronovich and Zavarotny* [2001] in the context of SSA-2. Thus, in this paper, for RCA, we consider that the first order term of the Volterra series in the scattering matrix expansion is a small perturbation in the phase term of the zeroth order contribution in Eq. () such as:

$$\mathbb{S}(\boldsymbol{k},\boldsymbol{k}_0)=\mathbb{K}_0(\boldsymbol{k},\boldsymbol{k}_0)\int_{\boldsymbol{r}} e^{-iQ_z\eta(\boldsymbol{r})}e^{-iQ_z\delta_{\boldsymbol{k},\boldsymbol{k}_0}\eta(\boldsymbol{r})}e^{-i\boldsymbol{Q}_H\cdot\boldsymbol{r}}d\boldsymbol{r}, \tag{10}$$

with

$$\delta_{\boldsymbol{k},\boldsymbol{k}_0}\eta(\boldsymbol{r})=\int_{\boldsymbol{\xi}}\frac{T_{\mathrm{lca/rca}}(\boldsymbol{k},\boldsymbol{k}_0;\boldsymbol{\xi})}{\mathbb{K}(\boldsymbol{k},\boldsymbol{k}_0)}\hat{\eta}(\boldsymbol{\xi})e^{i\boldsymbol{\xi}\cdot\boldsymbol{r}}d\boldsymbol{\xi}. \tag{11}$$

$\tilde{\eta}(\boldsymbol{r})=\eta(\boldsymbol{r})+\delta_{\boldsymbol{k},\boldsymbol{k}_0}\eta(\boldsymbol{r})$ can be seen as a modified surface elevation. In the case of RCA, the first order curvature term is applied on the small resonant waves responsible of the Bragg scattering mechanism according to SPM-1 theory. Thus, the simplification of the scattering matrix expansion to describe the contribution of the curvature correction term through a phase modification is consistent with the small perturbation hypothesis.

Using the modified surface elevation for the statistical derivation of the NRCS, in the Kirchhoff integral, the characteristic function $< e^{\eta} >$ is replaced by $< e^{\tilde{\eta}} >$. Under Gaussian statistics, this formalism enables to have a tractable expression for the NRCS:

$$\sigma_0^{pq}(\theta,\phi)=\left|\frac{\mathbb{K}(\boldsymbol{k},\boldsymbol{k}_0)}{Q_z}\right|^2 e^{-Q_z^2\tilde{\rho}(0)}\int_{\boldsymbol{r}}\left[e^{-Q_z^2\tilde{\rho}(\boldsymbol{r})}-1\right]e^{-i\boldsymbol{Q}_H\cdot\boldsymbol{r}}d\boldsymbol{r}, \tag{12}$$

with:

$$\tilde{\rho}(\boldsymbol{r})=\int_{\boldsymbol{\xi}}\left|1+\frac{T_{\mathrm{lca/rca}}(\boldsymbol{k},\boldsymbol{k}_0,\boldsymbol{\xi})}{\mathbb{K}(\boldsymbol{k},\boldsymbol{k}_0)}\right|^2 S(\boldsymbol{\xi})e^{i\boldsymbol{\xi}\cdot\boldsymbol{r}}d\boldsymbol{\xi}. \tag{13}$$

$\tilde{\rho}(\boldsymbol{r})$ is the so-called modified correlation function of a filtered spectrum and $S(\boldsymbol{\xi})$ the sea surface elevation spectrum. In the following, we use this formulation.

4. Results and Discussion

4.1. With Gaussian statistics for the sea surface description

As a first comparison between data and model, we present the PR versus incidence angle given by RCA, LCA-1 and KA for a 10m/s wind speed in C- and Ku-band in the case of an isotropic sea surface on figures 2 (a) and 2 (b). In both cases, we observe that the curvature correction term in RCA or LCA-1 ensures to the extended KA to get polarization sensitivity as the incidence increases. As expected, since the curvature correction term in RCA is restricted to the resonant Bragg waves, the induced polarization sensitivity is less than for LCA-1. From the data comparisons in Ku and C band presented here, we have a better agreement with RCA than with LCA-1. Figure 2 (c) presents the PR predicted by RCA and SSA-1 versus incidence angle for three frequencies. Focusing on the frequency dependency, we observe that the PR decreases when the frequency increases with both models. For SSA-1 (same comments can be done with KA or SPM-1) the only frequency dependency comes through the Kernel definition and is too small. In LCA-1 or RCA, the surface description controls the PR. This ensures, by construction, to reach dynamically both SPM-1 and KA asymptotic solutions, lead to KA results when $k_0 \to \infty$ or when the perception of the surface by the sensor is flat (no curvature). Numerical computations of the PR show that the RCA solution is more frequency sensitive than SPM-1, SSA-1 or KA. This explains why the model agrees well with the data in both Ku and C bands on figures 2 (a) and 2 (b).

As already mentioned above, another important feature in the backscattered signal for a given polarization, is the azimuth modulation with respect of the wind direction relative to the radar's azimuth look direction. From this modulation, we can infer the wind direction. Moreover, data analysis show that this modulation is incidence angle and frequency dependent. Most of electromagnetic models are able to reproduce these two dependencies. If this modulation is quite well reproduced in each co-polarization, it is not sufficient as the predicted modulation is not polarization sensitive (or not sufficiently for TSM). The comparison on figure 1 shows it. On figures 3 (a) and 4 (a), we present PR measured with STORM data for two cases of different wind speeds (11 and 14 m/s). These measurements exhibit an azimuth modulation dependent on the wind direction. To show the impact of the curvature model family, we present the results given by LCA-1 and RCA. As an example we also plot the SSA-1 results. LCA-1/RCA formalism enables to reproduce an azimuth modulation for the PR due to the curvature correction term. More precisely, following our hypothesis on Gaussian statistics for the sea surface representation, such kind of model can only reproduce the first order harmonic of the PR. We will see in the next section that this issue can be improved considering skewness effect. Comparisons between LCA-1 and RCA confirms that the mean level of the PR is better reproduced by RCA. The curvature effect attributed to the resonant waves provides also a better trend for the azimuth modulation amplitude. Figures 3 (c-d) and 4 (c-d) presents the NRCS in both VV and HH polarizations separately for these two wind speeds which are the direct measurable quantities. As expected from our previous conclusion (see figures 2), RCA predicts a correct mean level for the NRCS in both HH and VV polarizations whereas LCA and SSA-1 underestimate the NRCS in HH. As for the PR, due to Gaussian statistics, the three models only reproduce a first order harmonic modulation. However, with the curvature effect, this modulation is polarization sensitive. This fundamental aspect enables to predict a PR sensitive to geophysical parameters such as wind speed or wind direction relative to the radar's azimuth look direction. To be really complete with these data comparisons in C-band, we present on figure 3 (b) and 4 (b) the difference of NRCS $\sigma_0^{vv} - \sigma_0^{hh}$ in linear unit, DP hereafter, versus the wind direction relative to the radar's azimuth look direction for the two wind speeds considered here. Once again, RCA model is in better agreement with the data than other models. DP quantity is interesting since in literature, authors proposed to decompose the measured NRCS in a polarized and a scalar part (e.g. [*Quilfen et al.*, 1999]). Using DP quantity, we remove the scalar contribution to keep only the polarized part of the signal. In the case of backscattering, this part is taken into account through the first order curvature correction term in LCA/RCA formalism. As the comparisons with data are also satisfying for the DP quantity, we are confident in the first order resonant curvature term of RCA.

To evaluate the ability of RCA to reproduce the data for different incident wavelengths, we also present a set of comparisons in X-Band. These data were collected during POLRAD'96 experiment. The wind speed considered here was provided by buoys, ships and/or model. The data set and the instrument were presented in details by *Hauser et al.* [1997]. On the figure 5, as for STORM data, we present the PR (a), DP (b) and the NRCS (c-d) in both co-polarizations. In this case, from buoys and ship measurements, the wind speed is approximatively 8 m/s (we consider the mean of the four available measurements). As we already concluded for the C-Band, RCA/LCA formalism enables to reproduce an azimuth modulation for the PR. RCA predictions give a better agreement with the data than any of the other models presented in this paper.

These good agreement between RCA model and the data in C- and X- Band for the different sets of four comparisons has to be seen as a cross-validation of the RCA model as it would be easy to resolve only one aspect of the NRCS models but destabilizing an other. The consistency between RCA with data on these four aspects, where SSA-1, LCA-1 or KA fails (at least on one of these aspects), show the robustness of the model.

4.2. On the skewness effect on the NRCS

In all the data presented here, we observe a difference between the NRCS levels observed upwind and downwind. This asymmetry (UDA hereafter) was already evidenced by many authors thanks to radar data and is taken into account in the standard three-term Fourier model used for empirical formulations of the NRCS versus viewing angle with respect to wind direction (e.g. [*Stoffelen and Anderson*, 1997; *Bentamy et al.*, 1999; *Herbasch*, 2003]). Measurements, reveal that the NRCS level in upwind direction is greater than in downwind direction at high incidence angles (say $> 30°$) and lower at small incidence angles. In empirical models such as CMOD type models in C-Band or SASS in Ku-Band, the a_1 coefficient (see Eq.) takes into account this second order effect in the azimuth modulation. In physical models, a standard explanation for this asymmetry is done through the hydrodynamic modulation of Bragg waves. However, data analysis combining the dual co-polarization to remove the so-called scalar contribution thanks to the DP quantity firstly performed by *Chapron et al.* [1997] reveal that the contribution of the Bragg waves to the backscattered signal is more important downwind whereas the total contribution of the total UDA predicts more signal upwind. This analysis proves that if the hydrodynamic modulation of Bragg waves exists, its effect is dominated by an other one. Indeed, the slopes of the longer waves are more steep leeward than windward. On the longer waves slopes, the lower amplitude Bragg waves are predominantly windward. On the windward side, the longer waves may be slightly steeper and rougher to decrease the polarized contribution. This explains the observed UDA in the DP signal. Moreover, this implies that the opposite contribution of the UDA comes through the skewed form of the longer and the breaking waves which participate to the backscattering through the Kirchhoff mechanism. This idea consisting in associating the UDA of the breakers in a NRCS model was firstly applied by *Kudryavtsev et al.* [2003]. Same kind of dual co-polarizations analysis than the one performed by *Chapron et al.* [1997] or *Quilfen et al.* [1999] was proposed by *Mouche et al.* [2006b] in C-Band. This study based on STORM data for observations and *Kudryavtsev et al.* [2003] model also supports the idea of the breaking waves importance for the UDA through a scalar contribution to the NRCS.

Thus, we need to consider higher moments in the statistical derivation of the NRCS. The third order correction to the characteristic function enables to consider the skewness effect of the waves. In the local frame of RCA model, the modified characteristic function up to the third order is simply:

$$< e^{jQ_z(\tilde{\eta}_2-\tilde{\eta}_1)} > \approx e^{-Q_z^2(\tilde{\rho}(0)-\tilde{\rho}(\boldsymbol{r}))} e^{iQ_z^3 \tilde{S}_{\text{skew}}(\boldsymbol{r})}, \tag{14}$$

where $\tilde{S}_{\text{skew}}$ is the skewness function associated to the modified surface height function. According to RCA formalism it is clear that any correcting order of the characteristic function can be polarization and frequency dependent. Following this idea, the NRCS when considering the skewness effect is:

$$\sigma_0(\theta,\phi) = \left|\frac{\mathbb{K}(\boldsymbol{k},\boldsymbol{k}_0)}{Q_z}\right|^2 e^{-Q_z^2\tilde{\rho}(0)} \int_{\boldsymbol{r}} \left[e^{-Q_z^2\tilde{\rho}(\boldsymbol{r})+iQ_z^3\tilde{S}_{\text{skew}}(\boldsymbol{r})} - 1\right] e^{-i\boldsymbol{Q}_H\cdot\boldsymbol{r}} d\boldsymbol{r}. \tag{15}$$

In this work we choose for the skewness function a generic formulation as proposed by *Elfouhaily* [1997] adjusted on surface slope skewness when $\boldsymbol{r} \to 0$ [*Cox and Munk*, 1954]:

$$S_{\text{skew}}(\boldsymbol{r}) \underset{\boldsymbol{r}\to 0}{=} -\frac{1}{6}x\sigma_{sx}(x^2\sigma_{sx}^2 C_{03} + 3y^2\sigma_{sy}^2 C_{21}) \approx -\frac{r^3}{6}\sigma_{sx}^3 C_{03}\cos(\phi), \tag{16}$$

$$S'_{\text{skew}}(0) = S''_{\text{skew}}(0) = S'''_{\text{skew}}(0) = 0 \tag{17}$$

where ϕ is the angle of the wind direction relative to the radar's azimuth look direction and C_{03}, C_{21} two empirical coefficients given by *Cox and Munk*'s measurements [*Cox and Munk*, 1954].

On the figure 6 (a-f), we present the UDA asymmetry of the NRCS in both-co-polarizations and of the PR as measured with STORM radar and compared with the prediction of RCA model when considering the skewness effect. To complete the data set, we also show the UDA given by two empirical models CMOD-IFREMER [*Bentamy et al.*, 1999] and CMOD-5 [*Herbasch*, 2003]. Data indicates that the asymmetry is incidence, wind speed and polarization dependent. Results given by the RCA model give very good agreements with data. In particular, RCA is able to predict realistic and different UDA for VV and HH polarizations. As a direct consequence, the predicted UDA for the PR is also in agreement with the data. In Ku Band, we compare directly the $a1$ coefficient in linear scale for a 10 and 15m/s wind speed. We observe on figure 7 that the trend with incidence angle is rather well reproduced by the model thanks to the third order correction in the characteristic function.

Taking into account the skewness according to Eq. () alos modifies the azimuth modulation. To see the impact on the whole azimuth range, we present the same plot as on figure 8 where the model is compared to radar data acquired versus azimuth angle. The results from RCA are obtained with and without skewness effect. We observe that the third order correction gives more realistic trends for the NRCS with azimuth angles, as it adds a significant second order azimuthal modulation. As observed and predicted, this effect is greater in HH than in VV polarization.

5. Conclusion

We used recent improvements obtained in the field of electromagnetic scattering wave theories from random rough surfaces to consider the sea surface curvature influence on the radar backscatter measurements. LCA-1 and RCA were applied to the case of scattering from a 2-Dimensional sea surface and compared with other existing models. Comparisons with data showed that RCA results are in better agreement with the data whereas LCA results are very close to the TSM predictions. This difference between the two models comes from the fact that the RCA only takes into account the curvature effect of the resonant Bragg waves to the NRCS prediction.

The formalism of LCA/RCA has the advantage to take into account the depolarization effect of the sea surface through a dynamical term which depends on both the configuration of the instrument (incidence, frequency and polarization) and the sea surface curvature properties. This is a key element for an improved understanding of the electromagnetic and oceanic waves interactions. In the framework of RCA, the first order term enables to reproduce the NRCS in both co-polarization versus incidence angle in the microwave domain. Good agreements for each polarization allows the model to reproduce the mean PR. This leads to conclude that the curvature correction impact on the polarization is certainly necessary. From our knowledge, RCA is the only asymptotic electromagnetic theory applied to a 2-dimensional sea surface able to reproduce these results. Satisfying solutions, in term of results, are given by *Kudryavtsev et al.* [2003] and *Kudryavtsev et al.*

[2005] who proposed a semi-empirical model based on an explicit decomposition of the sea surface. In this model, the sea surface is separated in two parts. First, a regular one which is responsible for the specular reflection near nadir and for the Bragg scattering of short modulated waves by longer one through a TSM (which means also a separation of the scales for this regular part). Second, zones with enhanced roughness due to effect of breaking waves on the sea surface which produce a scalar contribution to the NRCS through specular reflection on theses steep slopes. Obviously a parallel between these approaches can be done as the zeroth order of RCA could be compared to the breaking waves and longer waves contribution invoked by *Kudryavtsev et al.* [2003] and *Kudryavtsev et al.* [2005] while the curvature correction term and the Bragg contribution could be associated to the same scattering process of the short resonant waves. Advantages of RCA are of course the absence of any dividing parameter to separate scales of the sea surface. Moreover, as the enhanced roughness zones contribution may be hard to precisely parameterize, it could be convenient to use a model such as RCA which consider both contributions from regular and non-regular surface implicitely through the characteristic function. In a future work, an explicit comparison of these two models will be done. But as an important issue, it can be stated that PR modulations shall follow the roughness distribution and disturbations.

Finally, we discussed the implication of the non Gaussian statistics on the NRCS for the sea surface description. Interestingly, it appears from RCA formalism that the characteristic function of the scattered field is polarization, incidence and frequency dependent. Moreover, RCA is in agreement with *Chapron et al.* [2003] conclusion about the UDA of the Bragg waves and breaking waves at large incidence angle. Taking into account a third order correction term in the characteristic function as a signature of breaking waves, it appears that extraction of the third moment in the backscattered signal would be interesting to improve our understanding of the impact of breaking events on the NRCS.

A model such as RCA can be used to improve our understanding about the backscatter signal modulations. As an example, since at large incidence angles the NRCS in HH is lower than the prediction of KA whereas it is the contrary for the VV polarization, it can simply be concluded that the sensor is very sensitive to the small waves in VV polarization (more backscattered signal) whereas for HH polarization it is the contrary (less backscattered signal) which means that the sensor is more sensitive to the longer and steeper waves in this configuration. At large incidence angles, such a large sensitivity to the longer and steeper waves than to the resonant Bragg waves will induces a larger Doppler shift associated to the remote sensed waves than in VV polarization. Next, this model will be used to derive an imaging radar model based on the correlation function modulation to interpret the variation of the NRCS due to changes in the geophysical parameters. This will help to define a more consistent combined analysis between measured Doppler shifts and backscatter signals.

Acknowledgments. (Text here)

Appendix A: NRCS expression of existing in the case of Gaussian statistics

For convenience, we recall here the expression of the NRCS for SPM-1, TSM, SSA-1 and KA models as they are used through the paper. The derivation is done in case of Gaussian statistics. We consider the same coordinates system and definitions than those used to expresse the RCA solution in section 3 but also in the review on approximated wave scattering theories from random rough surfaces proposed by *Elfouhaily and Guérin* [2004]. $\boldsymbol{K} = (\boldsymbol{k}, q_k)$ and $\boldsymbol{K}_0 = (\boldsymbol{k}_0, -q_0)$ respectively denotes the wave numbers of the scattered and incident waves. $\mathbb{B}(\boldsymbol{k}, \boldsymbol{k}_0)$ and $\mathbb{K}(\boldsymbol{k}, \boldsymbol{k}_0)$ are the so-called kernels of Bragg and Kirchhoff Approximations. Their expression can be found in [*Elfouhaily et al.*, 2003b]. $\boldsymbol{Q}_H = \boldsymbol{k} - \boldsymbol{k}_0$ and $Q_z = q_k + q_0$.

A1. Small Perturbation Method at first order

$$\sigma_0^{BR} = |\mathbb{B}(\boldsymbol{k}, \boldsymbol{k}_0)|^2 S(\boldsymbol{Q}_H) \tag{A1}$$

A2. Two Scale Model

$$\sigma_0^{TSM} = \int_{-\infty}^{\infty} d(\tan\Psi) \int_{-\infty}^{\infty} d(\tan\delta) \sigma_0^{BR}(\theta_i) P(\tan\Psi, \tan\delta), \tag{A2}$$

where $P(\tan\Psi, \tan\delta)$ is the joint probability density of slopes for the long waves, θ_i the local angle, and $\sigma_{0_{BR}}$ the NRCS given by the SPM-1 due to the small roughness elements modulated by the longer waves. In our calculation this probability density is assumed Gaussian. The calculation of $\sigma_{0_{BR}}$ is done considering the angles corrections given by *Elfouhaily et al.* [1999] instead of initial Valenzuela's results [*Valenzuela*, 1978]:

$$\theta_i = -\cos^{-1}[\cos(\theta + \Psi)\cos(\tan^{-1}\delta\cos\Psi)]$$

with $S_x = \tan\Psi$ and $S_y = \tan\delta$,

the slopes of longer waves in and perpendicular to the incident plane.

A3. Small Slope Approximation at first order

$$\sigma_0^{SSA-1} = \left|\frac{\mathbb{B}(\boldsymbol{k},\boldsymbol{k}_0)}{Q_z}\right|^2 e^{-Q_z^2\rho(0)} \int_{\boldsymbol{r}} \left[e^{-Q_z^2\rho(\boldsymbol{r})} - 1\right] e^{-i\boldsymbol{Q}_H\cdot\boldsymbol{r}} d\boldsymbol{r}. \tag{A3}$$

A4. Kirchhoff Approximation

$$\sigma_0^{KIR} = \left|\frac{\mathbb{K}(\boldsymbol{k},\boldsymbol{k}_0)}{Q_z}\right|^2 e^{-Q_z^2\rho(0)} \int_{\boldsymbol{r}} \left[e^{-Q_z^2\rho(\boldsymbol{r})} - 1\right] e^{-i\boldsymbol{Q}_H\cdot\boldsymbol{r}} d\boldsymbol{r}. \tag{A4}$$

References

Bentamy, A., P. Queffelou, Y. Quilfen, and K. Katsaros, Ocean surface wind fields estimated from satellite active and passive microwave instruments, *IEEE Trans. on Geosc. and Remote Sens.*, *37*, 2469–2486, 1999.

Berman, D., and D. Dacol, Manifestly reciprocal scattering amplitudes for rough surfaces interface scattering, *J. Acous. Soc. of Am.*, *87(5)*, 1990.

Chapron, B., V. Kerbaol, and D. Vandermark, A note on relationships between sea-surface roughness and microwave polarimetric backscatter measurements: results form polrad'96, *Proc. Int. Workshop POLRAD'96*, pp. 55–64, 1997.

Chapron, B., F. Collard, and V. Kerbaol, Satellite synthetic aperture radar sea surface doppler measurements, *Proc. of the 2nd Workshop on Coastal and Marine Applications of SAR, ESA SP-565*, pp. 133–140, 2003.

Chapron, B., F. Collard, and F. Ardhuin, Direct measurements of ocean surface velocity from space: Interpretation and validation, *J. Geophys. Res.*, *110(C07008)*, 2005.

Cox, C., and W. Munk, Measurements of the roughness of the sea surface from photogrphs of the sun's glitter, *J. Opt. Soc.*, *44(11)*, 838–850, 1954.

Elfouhaily, T., *A consistent wind and wave model and its application to microwave remote sensing of the ocean surface*, Thesis dissertation. Denis Diderot university - Paris 7, France, 1997.

Elfouhaily, T., and C.-A. Guérin, A critical survey of approximate scattering wave theories from random rough surfaces, *Waves In Rand. Media*, *14(4)*, R1–R40, 2004.

Elfouhaily, T., B. Chapron, K. Katsaros, and D. Vandermark, A unified directionnal wave spectrum for long and short wind-driven waves, *J. Geophys. Res.*, *102*, 15,781–15,796, 1997.

Elfouhaily, T., D. Thompson, D. Vandemark, and B. Chapron, A new bistatic model for electromagnetic scattering from perfectly conducting random surfaces, *Waves In Rand. Media*, *9*, 281–294, 1999.

Elfouhaily, T., S. Guignard, R. Awdallah, and D. Thompson, Local and non-local curvature approximation: a new asymptottic theory for wave scattering, *Waves In Rand. Media*, *13*, 321–337, 2003a.

Elfouhaily, T., M. Joelson, S. Guignard, and D. Thompson, Analytical comparison between the surface current integral equation and the second-order small slope approximation, *Waves In Rand. Media*, *13*, 165–176, 2003b.

Hauser, D., P. Dubois, and G.Caudal, Polarimetric wind-scatterometer measurements during polrad'96, *Proc. of Int. Workshop POLRAD'96*, pp. 55–64, 1997.

Hauser, D., T. Podvin, M. Dechambre, R. Valentin, G. Caudal, and J.-F. Daloze, Storm: A new polarimetric real aperture radar for earth observations, *Proc. of ESA POLinsar Int. Workshop*, 2003.

Herbasch, H., Cmod5 an improved geophysical model function for ers scatterometry, *ECMWF, Internal Report*, 2003.

Kudryavtsev, V., D. Hauser, G. Caudal, and B. Chapron, A semiempirical model of the normalized radar cross-section of the sea surface: 1. background model, *J. Geophys. Res.*, *108(C3)*, 2003.

Kudryavtsev, V., D. Akimov, J. Johannessen, and B. Chapron, On radar imaging of current features: 1. model and comparison with observations, *J. Geophys. Res.*, *110(C07016)*, 2005.

Monaldo, F., and V. Kerbaol, The sar measurement of ocean surface winds: An overview, *Proc. of the 2nd Workshop on Coastal and Marine Applications of SAR, ESA SP-565*, pp. 15–32, 2003.

Mouche, A., D. Hauser, J.-F. Daloze, and C. Guérin, Dual-polarization measurements at c-band over the ocean: Results from ariborne radar observations and comparison with envisat asar data, *IEEE Trans. on Geosc. and Remote Sensing*, *43(4)*, 753–769, 2005.

Mouche, A., B. Chapron, and N. Reul, A simplified asymptotic theory for ocean surface electromagnetic waves scattering, *Submitted to WRM*, 2006a.

Mouche, A., D. Hauser, and V. Kudryavtsev, Radar scattering of the ocean surface and sea-roughness properties: A combined analysis from dual-polarizations airborne radar observations and models in c band, *J. Geophys. Res.*, *111(C09004)*, 2006b.

Plant, W., A two-scale model of short wind-generated waves and scatterometry, *J. Geophys. Res.*, *91(C9)*, 10,735–10,749, 1986.

Plant, W., A stochastic, multiscale model of microwave backscatter from the ocean, *J. Geophys. Res.*, *107(C9)*, 2002.

Plant, W., Microwave sea return at moderate to high incidence angles, *Waves In Rand. Media*, *9*, 339–354, 2003.

Quilfen, Y., B. Chapron, A. Bentamy, J. Gourrion, T. Elfouhaily, and D. Vandermark, Global ers-1 and 2 nscat observations: Upwind/crosswind and upwind/downwind measurements, *J. Geophys. Res.*, *104(C5)*, 11,459–11,469, 1999.

Romeiser, R., W. Alpers, and V. Wismann, An improved composite surface model for the radar backscattering cross-section of the ocean surface: 1. theory of the model and optimization/validation by scatterometer data, *J. Geophys. Res.*, *102(C11)*, 25,237–

25,250, 1997.

Shaw, W., and A. Dougan, Green's function refinement as an approach to radar backscatter: General theory and application to lga scattering from the ocean, *IEEE Transaction on Antenna Propagation*, *46(1)*, 57–66, 1998.

Stoffelen, A., and D. Anderson, Scatterometer data interpretation: Estimation and validation of the transfer function cmod4, *J. Geophys. Res.*, *102*, 5767–5780, 1997.

Thompson, D., Calculation of radar backscatter modulations from internal waves, *J. Geophys. Res.*, *93(C10)*, 12,371–12,380, 1988.

Valenzuela, G., Theories for the interactions of electromagnetic and oceanic waves - a review, *Boundary-Layer Met.*, *13*, 61–85, 1978.

Voronovich, A., Small-slope approximation for electromagnetic wave scattering at a rough interface of two dielectric half-spaces, *Waves In Rand. Media*, *4*, 337–367, 1994.

Voronovich, A., and V. Zavarotny, Theoritical model for scattering of radar signals in ku- and c-bands from a rough sea surface with breaking waves, *Waves In Rand. Media*, *11*, 247–269, 2001.

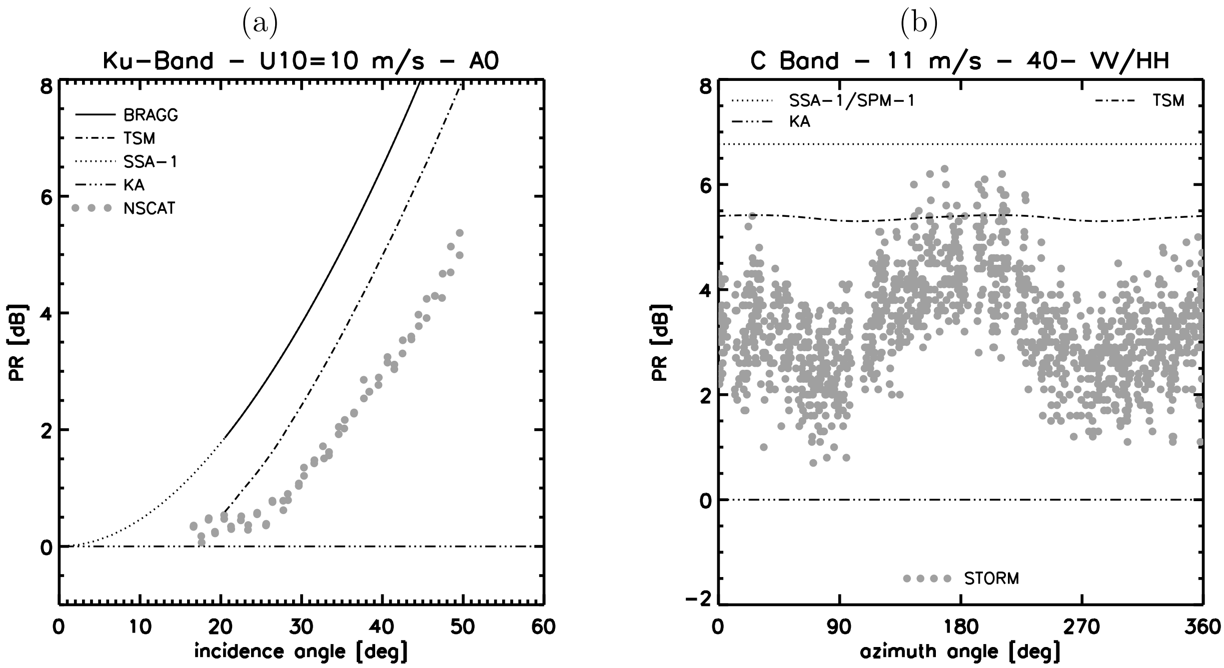

Figure 1. (a) Polarization ratio versus incidence angle in Ku band for a 10 m/s ten meters high wind speed in the case of an isotropic sea surface. (b) Polarization ratio versus wind direction relative to the radar's azimuth look direction for a 11 m/s ten meters high wind speed and a 40° incidence angle.

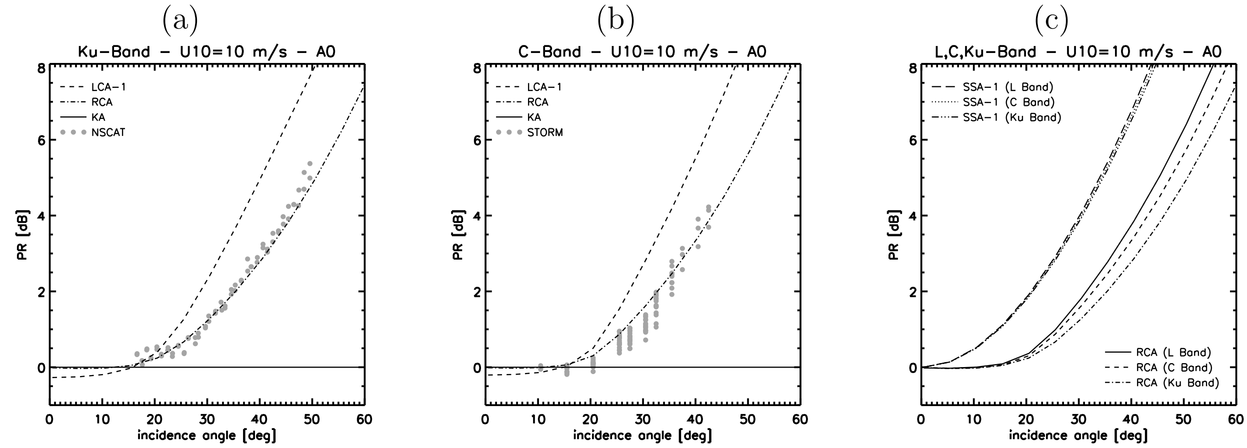

Figure 2. (a) Polarization ratio versus incidence angle in Ku band for a 10 m/s ten meters high wind speed in the case of an isotropic sea surface. Solid, dashed and dashed-dotted lines are respectively the predictions given by KA, LCA and RCA models. Data are from NSCAT. (b) Same than (a) but for C-Band. Data are from STORM radar. (c) Polarization ratio versus incidence angle for a 10 m/s ten meters high wind speed in the case of an isotropic sea surface in Ku, C and L Band given by RCA and SSA-1.

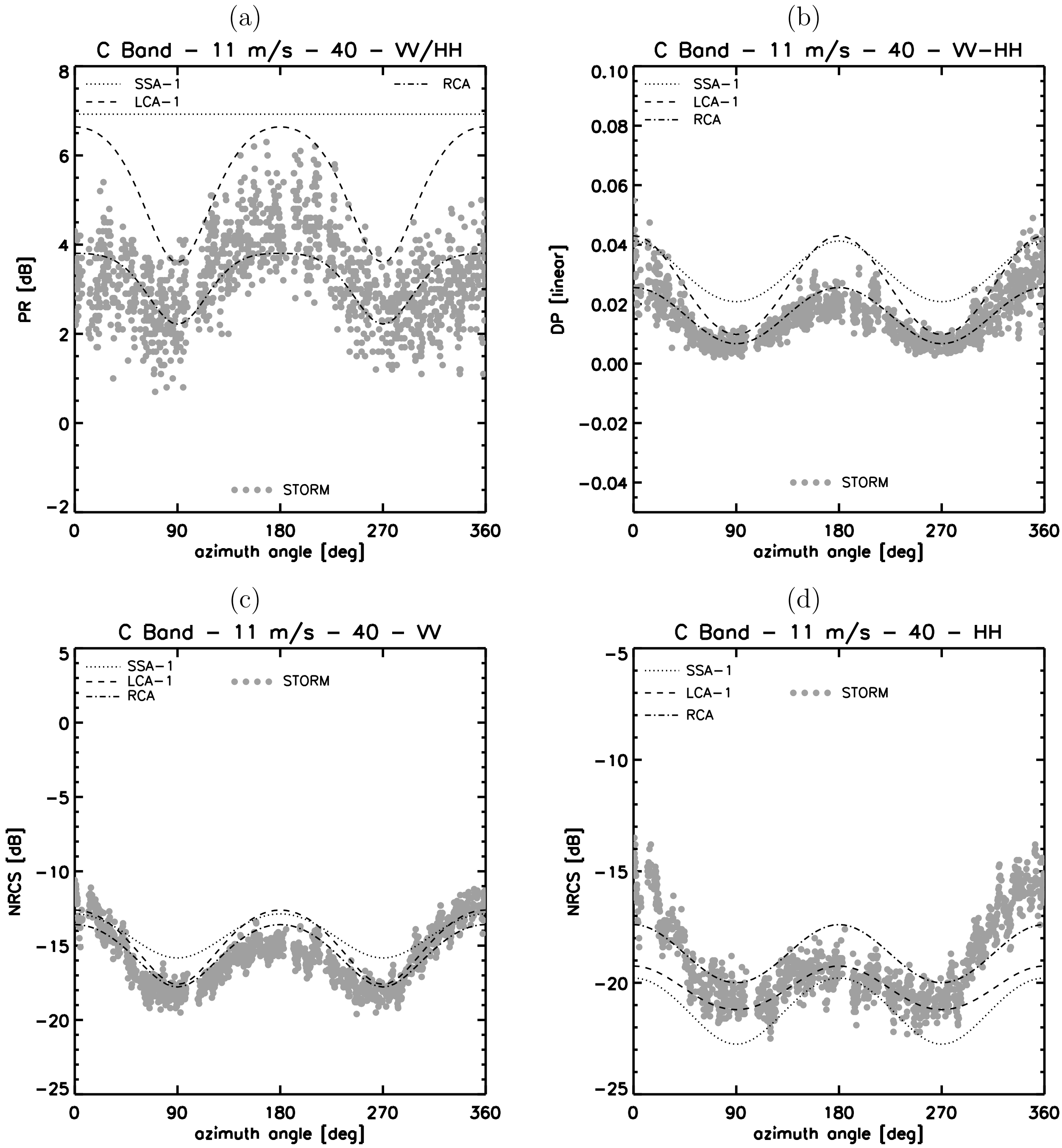

Figure 3. (a) Polarization ratio versus wind direction relative to the radar's azimuth look direction for a 11 m/s ten meters high wind speed, a 40° incidence angle in C band. (b) Same but for the difference of NRCS. (c) Same but for the NRCS in VV polarization. (d) Same but for the NRCS in HH polarization.

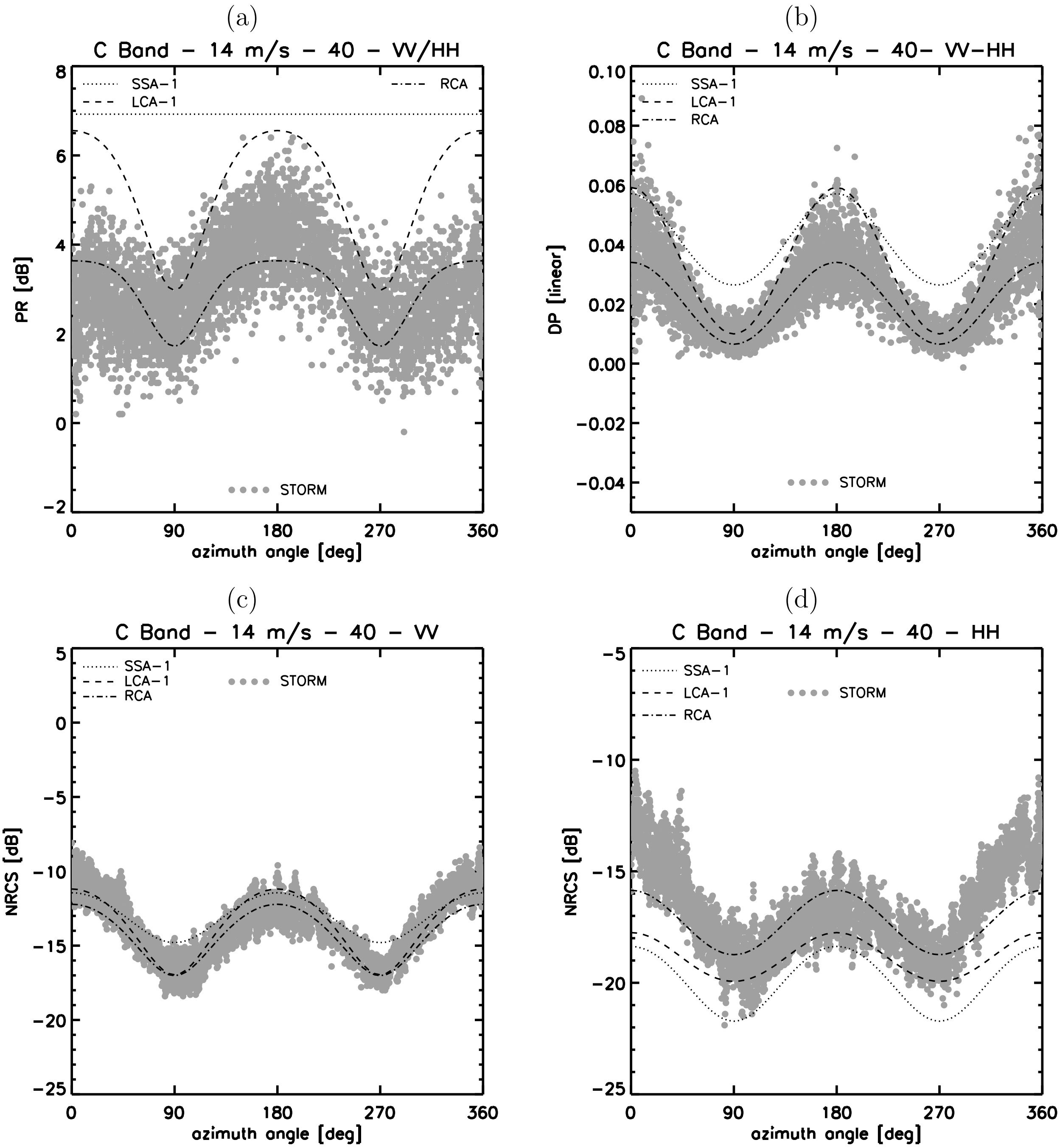

Figure 4. (a) Polarization ratio versus wind direction relative to the radar's azimuth look direction for a 14 m/s ten meters high wind speed, a 40° incidence angle in C band. (b) Same but for the difference of NRCS. (c) Same but for the NRCS in VV polarization. (d) Same but for the NRCS in HH polarization.

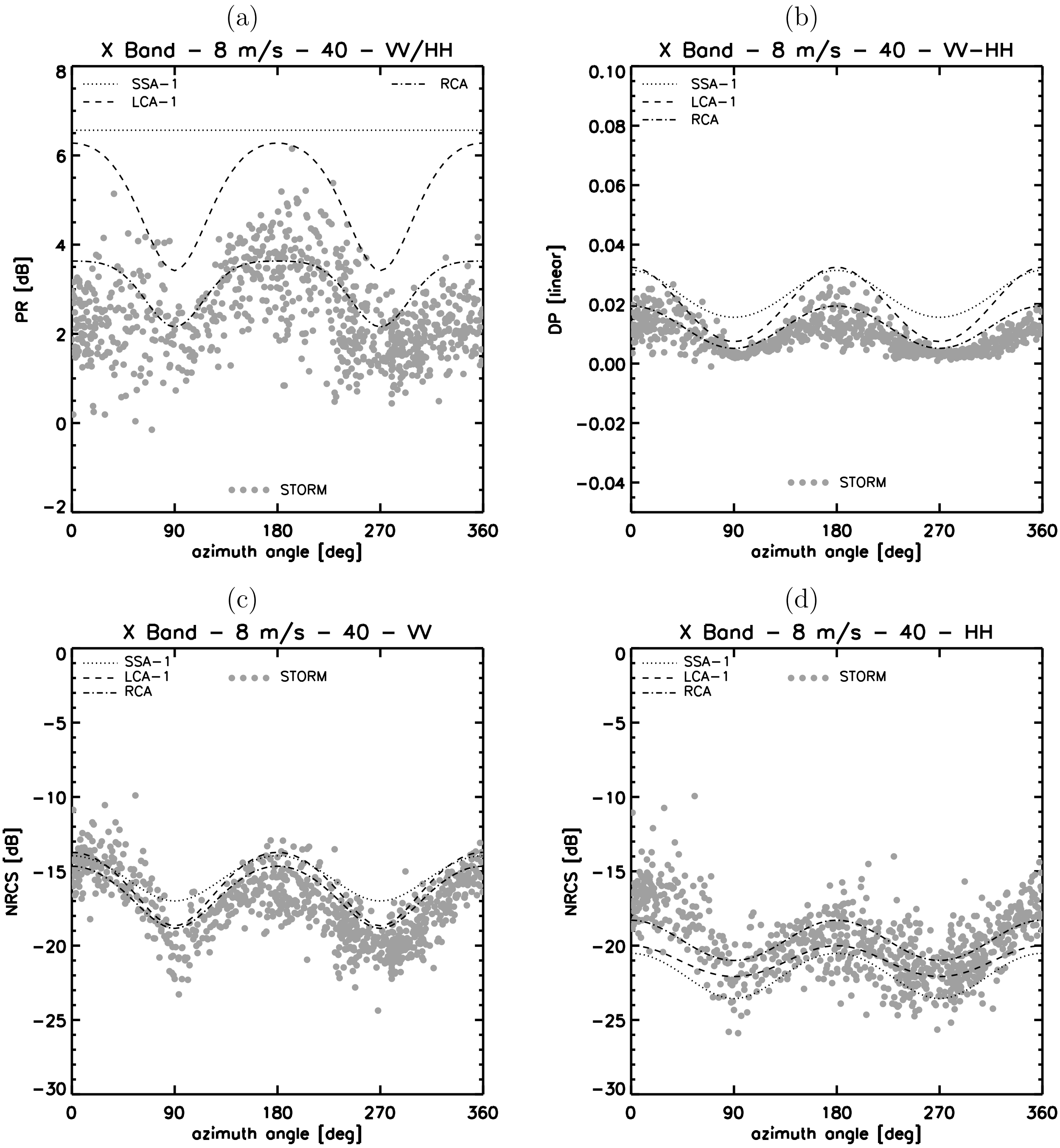

Figure 5. (a) Polarization ratio versus wind direction relative to the radar's azimuth look direction for a 8 m/s ten meters high wind speed, a 40° incidence angle in X band. (b) Same but for the difference of NRCS. (c) Same but for the NRCS in VV polarization. (d) Same but for the NRCS in HH polarization.

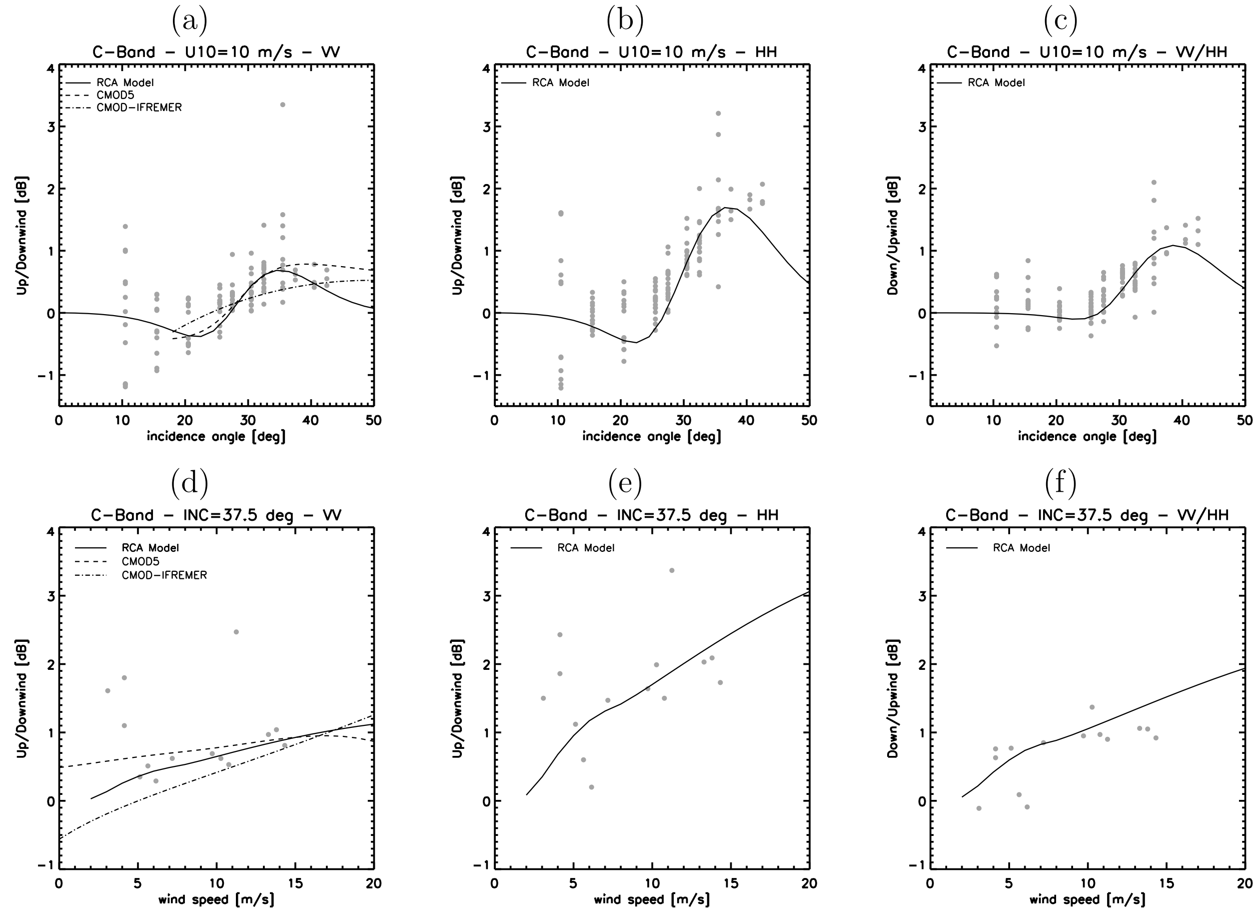

Figure 6. Top panel: UDA versus incidence angle in (a) VV and (b) HH polarizations for a 10m/s ten meters high wind speed. (c) Downwind to upwind asymmetry of the PR versus incidence angle for a 10m/s ten meters high wind speed. Bottom panel: UDA versus incidence angle for (a) VV and (b) HH polarizations for a 37.5° incidence angle. (c) Downwind to upwind asymmetry of the PR versus incidence angle for a 37.5° incidence angle

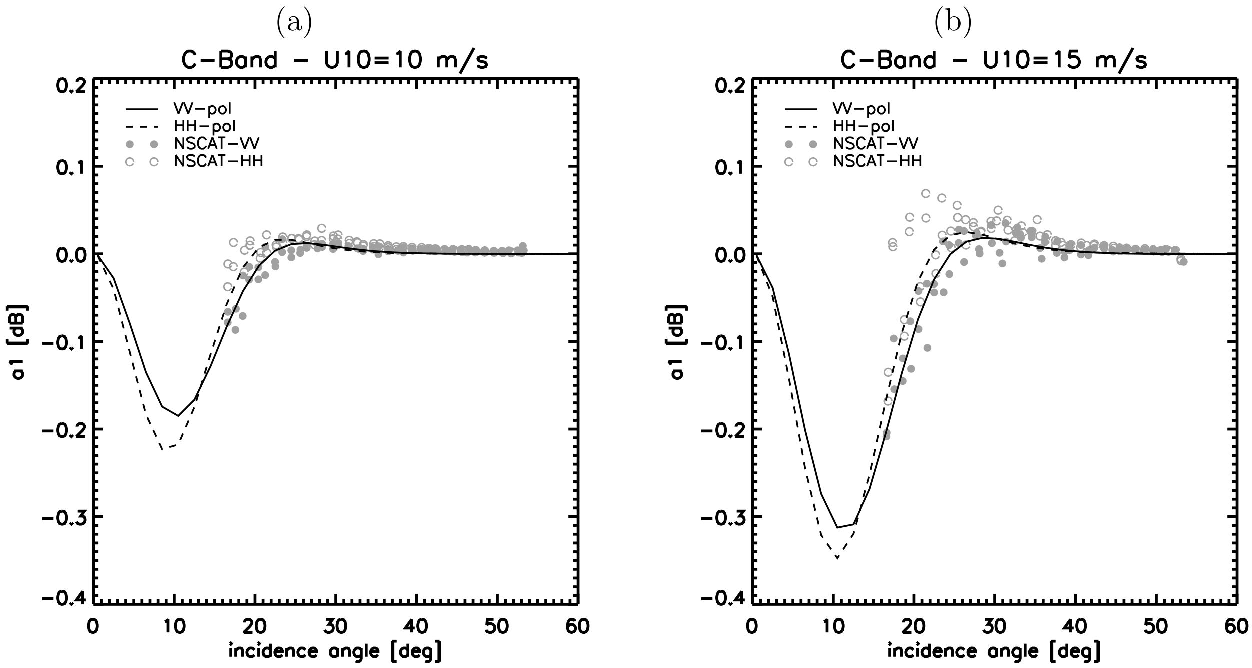

Figure 7. a_1^{vv} and a_1^{hh} coefficients as a function of the incidence angle in Ku-Band for two given ten meters high wind speeds: (a) 10m/s and (b) 10m/s.

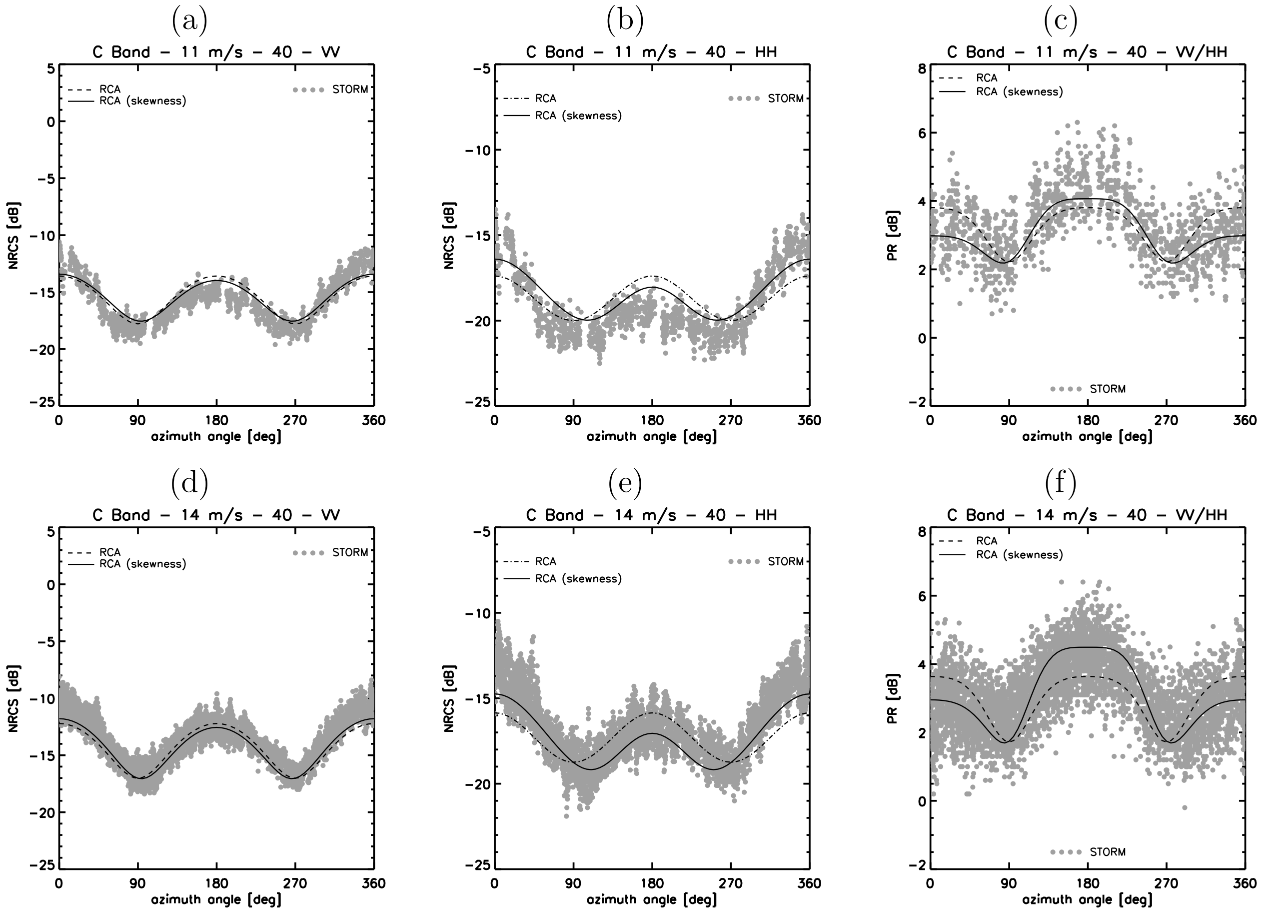

Figure 8. Top panel: NRCS versus wind direction relative to the radar's azimuth look direction for a 11 m/s ten meters high wind speed, a 40° incidence angle in C band in (a) VV and (b) HH polarizations. (c) Same for the PR. Bottom panel: NRCS versus wind direction relative to the radar's azimuth look direction for a 14 m/s ten meters high wind speed, a 40° incidence angle in C band in (a) VV and (b) HH polarizations. (c) Same for the PR.